within the sequence at positions 3 (Nap) and 6 (Bph in Br-Oct or Phe in C-Oct). The oligopeptides were characterized by ^{1}H NMR and FAB mass spectroscopy and purified by reverse-phase HPLC on a C_{18} column prior to all optical studies. ^{1}H NMR studies of the amide proton resonances of C-Oct showed a distinctive backbone hydrogen bonding pattern indicative of a 3_{10} helical conformation[18] in agreement with extensive similar studies of both pure Aib oligomers[11a] and Aib-rich polypeptides.[11c] Furthermore, circular dichroism spectra[19] of C-Oct measured in both methanol and acetonitrile indicated the presence of substantial helical secondary structure.[20]

Fluorescence. Both steady-state and time-resolved[21] fluorescence data have been obtained for C-Oct (no bromine) and Br-Oct (Table I). The fluorescence quantum yield of Br-Oct is observed to be a factor of 3 less than that of C-Oct in five solvents. The time-resolved data also unambiguously demonstrate fluorescence quenching by the remote bromine atom. It is especially interesting to compare the fluorescence quenching in the two brominated species, Br-Oct and Br-Dim. Remote heavy atom quenching is more than twice as effective in Br-Oct than in Br-Dim, even though the bromophenyl group is separated from the naphthalene by 13 σ bonds in Br-Oct and only seven σ bonds in Br-Dim (adjacent residues).[22] The addition of σ bonds would be expected to lower through-bond interactions. Despite the addition of six σ bonds, and the subsequent decrease in through-bond interactions, the octamer exhibits greater quenching than the dimer, demonstrating that noncovalent interactions exceed through-bond interactions in the helical octamer.[23]

Mechanism of Fluorescence Quenching. Intramolecular singlet exciplex formation can be ruled out as a mechanism of the quenching since the emission spectra of Br-Oct and C-Oct are identical in shape and the characteristic long-wavelength exciplex emission is absent.[24] Singlet–singlet energy transfer is also ruled out due to the lack of any absorption by bromobenzene at 290 nm or longer. The fluorescence yield of Br-Oct also exhibits a pronounced insensitivity to solvent dielectric constant (Table I), which is evidence against the possible involvement of a fast charge-transfer process in the mechanism of accelerated singlet-state decay.[25]

Nanosecond transient absorption spectroscopy of Br-Oct and C-Oct in acetonitrile demonstrated the formation of the Nap triplet state in both peptides. In addition, the transient spectrum of Br-Oct did not exhibit any absorption due to a Nap radical cation. The triplet yield of Br-Oct relative to C-Oct (Φ_T'/Φ_T) was measured to be (93 ± 3)%. This falls in between two simple limits: (i) Φ_T'/Φ_T = 32% (identical with the relative fluorescence yield, Table I) for a quenching mechanism that yields no additional triplets and (ii) $\Phi_T'/\Phi_T > 100\%$ for a mechanism that is exclusively enhanced intersystem crossing to the triplet. The triplet yield and biexponential time-resolved fluorescence data[21] taken together lead to a model with minor and major kinetic pathways. The Nap singlets of the minor components deactivate very quickly and not through accelerated intersystem crossing, whereas the quenching of the Nap singlets of the dominant component must be due to bromine-induced enhanced intersystem crossing ($S_1 \rightarrow T_1$). Triplet exciplex formation could be the minor pathway.[21] The dominant pathway is assigned to remote heavy atom induced intersystem crossing with a rate constant of 2.0×10^7 s^{-1} (see Table I).

Summary. Fluorescence studies on the bromine-containing peptides we have designed enable a new method for studying long-range electronic interactions in peptides. The results demonstrate that a remote heavy atom can effectively enhance the intersystem crossing in the naphthalene probe chromophore even when separated by 13 σ bonds and that it is possible for noncovalent interactions to play a dominant role in exchange interactions between aromatic residues within helical peptides. We are also currently engaged in parallel intramolecular electron transfer studies, based on the same helical Aib strategy, to further explore the electronic control of nonadiabatic reaction processes within molecular architectures.

Acknowledgment. The support of this work by the NIHGMS First Program (R29-GM39576) is most gratefully acknowledged. We are also indebted to M. Venu Gopal for assistance in the CD spectroscopic measurements. A.K. also thanks the NSF Presidential Young Investigator program (CHEM-8958514) for their valued support.

Supplementary Material Available: Detailed description and kinetic analysis of transient absorption and emission studies on C-Oct and Br-Oct (7 pages). Ordering information is given on any current masthead page.

(14) Bodanzky, M. *Principles of Peptide Synthesis*; Springer-Verlag: New York, 1984.

(15) (a) Vittorelli, P.; Heimgartner, H.; Schmid, H.; Hoet, P.; Ghosez, L. *Tetrahedron* **1974**, *30*, 3737. (b) Obrecht, D.; Heimgartner, H. *Helv. Chim. Acta* **1987**, *70*, 102. (c) Haveaux, B.; Dekoker, A.; Rens, M.; Sidani, A. R.; Toye, J.; Ghosez, L. In *Organic Syntheses*; Noland, W. E., Ed.; John Wiley and Sons: New York, 1988; Collect. Vol. VI, pp 282–289.

(16) Carpino, L. A.; Cohen, B. J.; Stephens, K. E., Jr.; Sadat-Aalaee, S. Y.; Tien, J.; Langridge, D. C. *J. Org. Chem.* **1986**, *51*, 3732.

(17) The conformation in the figure is one of 10 locally minimized structures observed in preliminary energy minimizations performed with potentials kindly provided by Dr. M. Dudek in the laboratory of Dr. H. A. Scheraga.

(18) Solvent perturbation studies (DMSO-d_6 added to CD_3CN) on C-Oct unambiguously demonstrated seven intramolecular H bonded amide protons (out of nine) characteristic of a 3_{10} H-bonding pattern. For related NMR studies, see ref 10a.

(19) For CD studies of polypeptides containing Nap, see: Sisido, M.; Imanishi, Y. *Macromolecules* **1986**, *19*, 2187.

(20) CD measurements were performed on an AVIV (Model 60DS) machine in the laboratory of Dr. B. A. Wallace: 50 μM samples of C-Oct in CH_3OH and CH_3CN exhibited an intense band at 225 nm ($\sim -3.0 \times 10^4$ deg cm^2 dmol^{-1} of mean residue ellipticity) which indicates a high degree of helicity.

(21) See supplementary material for details.

(22) Extended conformations of the dimer are most probable, as confirmed by 10 minimized conformations obtained from CHARMm and the lack of bromo dimer exciplex emission.

(23) The interaction tunneling matrix element $\Delta = |TS + TB|$ is the result of through-bond (TB) interactions and through-space (TS) interactions, by which is meant here all nonbonded mechanisms of interaction. It is important to appreciate that both mechanisms may be simultaneously operative. From the data on the octamers and dimers we can conclude that $\Delta_8 > \Delta_2$; so $|TS8 + TB8| > |TS2 + TB2|$. Now if we assume that $|TB2| \gg |TS2|$ and define n such that $n|TB8| = |TB2|$, we have $|TS8 + TB8| > |TB2|$, from which it follows that $|TS8| > |TB2| - |TB8|$ and hence $|TS8| > (n-1)|TB8|$, where n may be estimated purely by a through-bond model.

(24) A dramatic long-wavelength singlet exciplex emission was readily observed in solutions of bromobenzene and α-methylnaphthalene.

(25) For an example and discussion of a solvent insensitive *intermolecular* heavy atom effect, see ref 2b.

Oxygen Insertion in the Ni(II) Complexes of Dioxopentaaza Macrocyclic Ligands

Dian Chen and Arthur E. Martell*

Department of Chemistry, Texas A&M University
College Station, Texas 77843-3255

Received July 25, 1990

This communication reports a new type of model monooxygenase-type reaction involving activation of dioxygen through metal–dioxygen complex intermediates. Analysis of the ligand degradation products formed from the dioxygen adducts of the Ni(II) complexes of the macrocyclic ligands 1,4,7,10,13-pentaazacyclohexadecane-14,16-dione (**1**), 15-ethyl-1,4,7,10,13-pentaazacyclohexadecane-14,16-dione (**2**), and 15-benzyl-1,4,7,10,13-pentaazacyclohexadecane-14,16-dione (**3**) shows conversion of these ligands in good yield (85 ± 5%) to the corresponding 15-hydroxylated derivatives, **4–6**. This is the first example of the hydroxylation of an aliphatic ligand by a metal dioxygen complex, since all previous examples involve oxygen insertion into aromatic rings. These include activation of dioxygen in tyrosinase model systems reported by Karlin et al.[1] and by others,[2-4] involving the formation of binuclear dioxygen adducts

(1) Karlin, K. D.; Hayes, J. C.; Gultneh, Y.; Cruse, R. W.; McKown, J. W.; Hutchinson, J. P.; Zubietta, J. *J. Am. Chem. Soc.* **1984**, *106*, 2121.

0002-7863/90/1512-9411$02.50/0

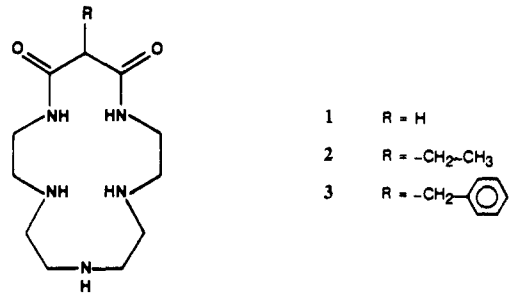

1 R = H

2 R = -CH_2-CH_3

3 R = -CH_2-

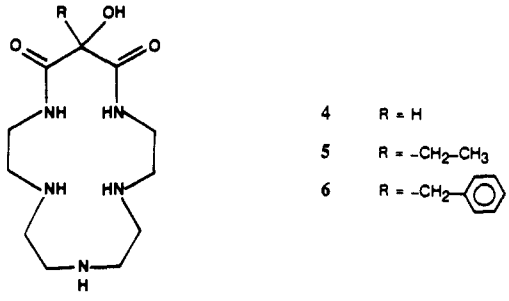

4 R = H

5 R = -CH_2-CH_3

6 R = -CH_2-

from Cu(I) complexes. Also, Kimura et al.[5,6] has reported hydroxylation of benzene, toluene, and anisole by nickel–dioxygen complexes.

Ligands **1–3** were synthesized by a modification of the method of Kimura et al.[7] and were characterized by ^{1}H NMR, mass spectra, and melting point. A detailed thermodynamic study ($\Delta G°$, $\Delta H°$, $\Delta S°$) of the formation of the 1:1 dioxygen complexes of the Ni(II) complexes of **1–3** will be published elsewhere.[8]

In order to identify the products resulting from the attack by activated dioxygen on the ligands of the nickel–dioxygen complexes, product analysis was carried out as follows. At 25.0 °C, 500 mg of the ligand and equimolar $NiCl_2 \cdot 6H_2O$ were added to 100 mL of 0.10 M borax buffer solution (pH 10.3) under anaerobic conditions to form the pale purple complexes ($NiH_{-2}L$), where L = **1**, **2**, or **3** and two amide hydrogen ions are displaced from the ligand. Air or dioxygen was then bubbled through the solution for 24–48 h, producing color changes from the initial pale purple to deep brown, and finally to yellow. A 2.0-g sample of solid ethylenediaminetetraacetic acid was added to the reaction mixture, with stirring, whereupon the pH dropped to 3.5. The pH was increased to 11 by addition of 50% NaOH solution, and the color changed to green (Ni(II)–EDTA). About 90% of the solvent water was removed by evaporation, and the residual solution was extracted three times with chloroform. The oxidized ligand was obtained as a white solid by evaporation of the chloroform solvent and was analyzed by ^{13}C NMR. The spectra of all three ligands had new strong resonances at 78.6, 80.5 and 87.7 ppm (relative to TMS) for **4–6**, respectively. These peaks are assigned to the group RCOH, where R = H, ethyl, and benzyl, respectively. For **4**, the ^{1}H NMR showed a new single resonance at 4.5 ppm, which disappeared after addition of D_2O, so that it represents the active H of RCOH. Mass spectra of the oxidized ligand gave the molecular ions 363 (**6**), 301 (**5**), and 273 (**4**), all of which are 16 mass units above those of the original ligands. These data clearly indicate the insertion of an oxygen atom in each of these ligands. NMR studies of the reaction products showed the yields to be 85 ± 5%, based on the amount of macrocyclic ligand employed.

In order to determine the source of oxygen in the insertion reaction, degradation product analysis was carried out on the Ni(II) complex of **3** in the same manner as the $^{16}O_2$ oxygenation products, but with $^{18}O_2$ as the only source of dioxygen. The mass spectral analysis gave a molecular weight of 365 (rather than 363 for the $^{16}O_2$ reaction), definitely demonstrating that the inserted oxygen came from the gaseous $^{18}O_2$ via the dioxygen complex.

The degradation rates of the three Ni(II)–dioxygen complexes are significantly different. For the Ni(II)–dioxygen complex of **1**, the dark brown color characteristic of the dioxygen complex lasted several (5–10) min. For the corresponding complex derived from **2**, it persisted for about 1 h, while for **3** it lasted 4 h. Thus the rates of degradation of the dioxygen complexes varied in the order **1** > **2** > **3**. This difference is ascribed to the protective and stabilizing effects of the alkyl and aralkyl groups on the corresponding dioxygen complexes. The Ni(II) complexes of the hydroxylated ligands showed no tendency to combine with dioxygen. It is suggested that the highly polar hydrophilic hydroxyl group in the ligand has a destabilizing effect on coordinated superoxide. This seems to be in accord with the stabilizing effect observed when the ligand is substituted at the same position by a hydrophobic alkyl or aralkyl group (as in **2** and **3**).

The high yields of hydroxylation products **4–6** indicate that oxygen insertion into the ligand is the main reaction pathway for oxygen activation in these nickel–dioxygen complexes. Although Kimura[5,6] found a loss of 40% of the nickel(II)–dioxygen complex in conversion of benzene to phenol under similar reaction conditions, the quantities of benzene employed and of phenol found were not reported. Because much or most of the loss of dioxygen complex may now be ascribed to ligand hydroxylation, there can be no doubt that aromatic hydroxylation is a minor hydroxylation pathway under the conditions employed (i.e., in aqueous solution) and that nearly all of the dioxygen activation is directed toward ligand hydroxylation. These results do not preclude, however, the possibility that aromatic substrate hydroxylation by these nickel(II) dioxygen complexes may turn out to be a major dioxygen activation pathway under entirely different reaction conditions (i.e., in aprotic low dielectric constant solvents).

Acknowledgment. This work was supported by a research contract with L'Air Liquide, S.A., Paris, France.

(2) Casella, L.; Rigoni, I. *J. Chem. Soc., Chem. Commun.* **1985**, 1668; Casella, L.; Gullotti, M.; Pollanze, G.; Rigoni, L. *J. Am. Chem. Soc.* **1988**, *110*, 4227.
(3) Gelling, O. J.; van Bolhuis, F.; Meetsma, A.; Feringa, B. I. *J. Chem. Soc., Chem. Commun.* **1988**, 552.
(4) Menif, R.; Martell, A. E. *J. Chem. Soc., Chem. Commun.* **1989**, 1521.
(5) Kimura, E.; Machida, R. *J. Chem. Soc., Chem. Commun.* **1984**, 499.
(6) Kimura, E.; Sakonaka, A.; Machida, R. *J. Am. Chem. Soc.* **1982**, *104*, 4255.
(7) Kimura, E.; Machida, R.; Kodama, M. *J. Am. Chem. Soc.* **1984**, *106*, 5497.
(8) Chen, D.; Motekaitis, R. J.; Martell, A. E. *Inorg. Chem.*, submitted.

Importance of Hydrogen Bond Acceptor Ability in Design of Host Molecules Capable of Molecular Recognition

K. M. Neder and H. W. Whitlock, Jr.*

Samuel M. McElvain Laboratories of Organic Chemistry
Department of Chemistry, University of Wisconsin
Madison, Wisconsin 53706

Received February 23, 1990
Revised Manuscript Received October 13, 1990

Use of pyridine units as hydrogen-bond (H-bond) acceptors in the design of host molecules is of current interest.[1-3] We report here that decreasing the pyridine basicity in hosts **1** can destroy the ability to complex H-bond, donating phenols (ρ −2.3).[4] From the molecular architecture perspective, the host–guest K_{assoc}

(1) (a) Chang, S.-K.; Hamilton, A. D. *J. Am. Chem. Soc.* **1988**, *110*, 1318. (b) Askew, B.; Ballester, P.; Buhr, C.; Jeong, K. S.; Jones, S.; Parris, K.; Williams, K.; Rebek, J., Jr. *J. Am. Chem. Soc.* **1989**, *111*, 1082. (c) Tucker, J. A.; Knobler, C. B.; Trueblood, K. N.; Cram, D. J. *J. Am. Chem. Soc.* **1989**, *111*, 3688. (d) Gutsche, C. D.; Alam, I. *Tetrahedron* **1988**, *44*, 4689.
(2) (a) Jarvi, E. T.; Whitlock, H. W. *J. Am. Chem. Soc.* **1982**, *104*, 7196. (b) Adams, S. P.; Whitlock, H. J. *J. Am. Chem. Soc.* **1982**, *104*, 1002. (c) Adams, S. P.; Whitlock, H. W. *J. Org. Chem.* **1981**, *46*, 3474.
(3) (a) Whitlock, B. J.; Whitlock, H. W. *J. Am. Chem. Soc.* **1990**, *112*, 3910. (b) Sheridan, R. E.; Whitlock, H. W., Jr. *J. Am. Chem. Soc.* **1986**, *108*, 7120. (c) Sheridan, R. E.; Whitlock, H. W., Jr. *J. Am. Chem. Soc.* **1988**, *110*, 4071. (d) Sheridan, R. E. Ph.D. Thesis, University of Wisconsin, Madison, WI, 1988.
(4) (a) Hamilton, R. D.; Little, D. *J. Chem. Soc., Chem. Commun.* **1990**, 297. (b) Hamilton, A. D.; Van Engen, D. *J. Am. Chem. Soc.* **1987**, *109*, 5035.

0002-7863/90/1512-9412$02.50/0